

Is There a Threshold for PSB Formation in Iron

Chong Wang^{1,*}, Danièle Wagner, Claude Bathias

¹ LEME, University Paris Ouest Nanterre La Défense 50, rue de Sèvres, 92410 VILLE D'AVRAY, France

* Corresponding author: wangchongscu@163.com

ABSTRACT

Thin flat specimens (1mm thickness) have been tested on a piezoelectric fatigue machine in 20 KHz frequency on High cycle fatigue domain and beyond. The result shows that body centered cubic Armco iron (with 80ppm of carbon content) could fail after 10^9 cycles at a loading well below the yield stress. Observations under Scanning Electron Microscope on the specimen surface and the fracture surface indicated gigacycle fatigue failure originated in the specimen surface and related to the formation of Persistent Slip Bands (PSB). The microstructure evolution was observed by optical microscopy. It was found that PSB not only appear at the beginning of ultrasonic fatigue test but also increase with the number of cyclic loading.

Keywords Persistent Slip Band, irreversible deformation, localized plasticity, very high cycle fatigue

1. Introduction

For single phase materials without inclusions, testing in very high cycle fatigue regime, the first damage event of crack initiation is due to the occurrence of Slips Marks (SM) on the specimen surface [1, 2]. In f.c.c materials (which are the most studied materials), these SM are called Persistent Slips Bands (PSB), with a particular dislocation structure beneath the PSB [3]. When strain reached to cyclic stress-strain curve plateau, the deformation structure changes to the PSB instead of dislocation veins in matrix in order to accommodated the high value of plastic deformation [1]. Intrusions at PSB or PSB/matrix are interface preferential sites for the nucleation of microcracks[4]. In bcc materials, like Armco iron, the identification of these SM with PSB is matter of debate [3-9]. The reason lies in the very different temperature and strain rate dependent dislocation glide behavior in body centered cubic (b.c.c) metals, as compared to f.c.c metals. Moderate increase of temperature, low cyclic strain rates and alloying by substitution atoms (e.g. in Fe-Si) and interstitial atoms (e.g. C and N in α -iron) make the dislocation glide modes of bcc metals more similar to those of f.c.c metals and then, "PSBs" may be observed.

For a basic point of view, it is of interest to understand the initiation of a fatigue crack in the VHCF regime in pure alloys or metals without internal defects. Studies tested at different loading conditions given references for investigating fatigue features on iron. Dislocation arrangement in iron after fatigue bending test at low frequency are investigated by Mcgrath and Bratina[10]. They find that the average dislocation density for particular stress amplitude reaches a constant value after showing a rapid increase in the early portion of the fatigue life. When Wood et al [11] compare the fatigue mechanisms in bcc iron and fcc metals at low frequency in alternating

torsion, they noted that at amplitudes above the SN knee, slip markings appeared on a specimen after a few cycles. At amplitude below the knee they appeared after a million or so cycles. Wei and Baker found wall developed arrays of dislocation loops in iron specimen after only 10 cycles in push-pull fatigue [12]. Such observation at small number of cycles is difficult at high frequency in VHCF.

However, fatigue deformation features of iron at very high cycle fatigue regime are limited. PSBs formation at subsurface and at initiation area was not well discussed on literature. Current work intends to investigating the fatigue initiation and localized irreversibility of b.c.c. metals ARMCO iron (α -Fe) at very high cycle fatigue regime. In order to study this phenomenon a new flat specimen, easy for surface observation, was designed to be tested at 20 kHz up to 10^{10} cycles. Observations were performed on specimen surface during testing and fractographic after failure.

2. Experimental

The studied material is a polycrystalline α iron whose chemical composition is given in Table 1 and mechanical properties of corrected true stress-strain is given in Fig 1. The microstructure is ferrite with equiaxe grains. The ferrite grain size is included in 10 to 40 μm . No specifically orientation was observed by EBSD.

Table 1. Chemical compositions (wt.%)

C	P	Si	Mn	S	Cr	Ni	Mo	Cu	Sn	Fe
0.008	0.007	0.005	0.048	0.003	0.015	0.014	0.009	0.001	0.002	Balance

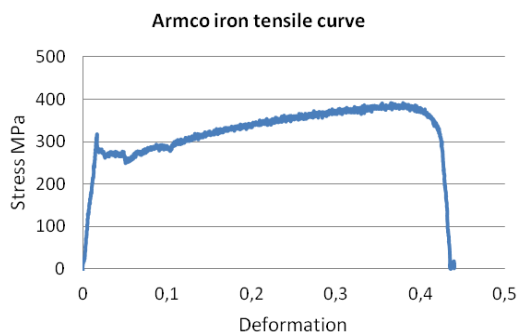


Fig 1. Stress-strain curve

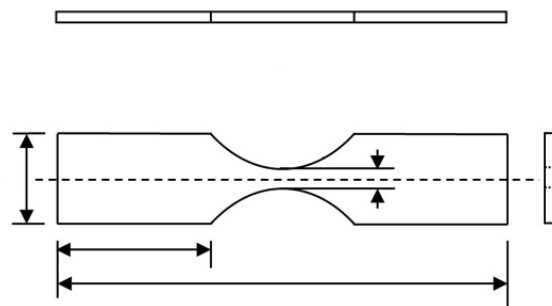


Fig 2. Sketch of flat ultrasonic specimen

For the reason of surface online observation condition by IR camera and optic microscope, a new design of 1 mm flat specimen (Fig. 2) was used to carry out fatigue tests. Specimen, special attachment and piezoelectric fatigue machine constituted the resonance system working at 20 kHz. The cyclic loading is tension-compression. The stress ratio is then $R = -1$. Before testing, both sides surface of the flat specimen were polished. One surface of the flat specimen was electrolytic etched.

According to specimen designs, the specimen center has zero axial displacement theoretically during ultrasonic fatigue loading. The displacement rises continually at positions both sides away from the center. There is a small area on the surface which includes specimen center remains visible by optical microscope because the displacement maintained at very low level. Therefore a mobile optical microscope constructed for taking the online image. It has magnification 320X and recording image at frequency up to 1 Hz. With this mobile optical microscope, it is possible to observe general appearance when character deformation takes place in the specimen surface like enforced slip bands. The typical online observation system is shown at Fig. 3.



Fig. 3 Experimental system

3. Results and discussions

By the advantage of displacement node and stress distribution at center of gigacycle fatigue specimen, with online optical microscope observation, Fig. 4 shows the evolution of irreversible deformation in the specimen surface by increasing number of cycles. It is found that, irreversible slip bands formed at the beginning of fatigue loading. This slip bands are multiplied or grown in the same grain due to following cycle loading. At neighbor area, new irreversible slip bands formed independently in another grain where no deformation appears at previous 1.6×10^7 cycles. Grain, either one already with slip band or one without slip band can have new slip band occurrence due to fatigue loading in same test condition. At the slip bands site where optical observation carried out, most of irreversible slip bands formed before 3×10^8 cycles. Only slightly evolution occurs by cyclic loading during fatigue life between 3×10^8 and 10^{10} cycles. Fig. 4 suggests that new irreversible deformation (localized plastic strain) per each loading cycle $\Delta \epsilon / N$ is decreasing with increasing number of cycle. $\Delta \epsilon / N$ closing to zero after 3×10^8 cycles in this case. In other words, crack initiation due to cumulating further new irreversible deformation after 3×10^8 cycles is scattered dispersed. That may be the reason why the S-N curve is normally significantly dispersed at regime beyond 10^9 cycles.

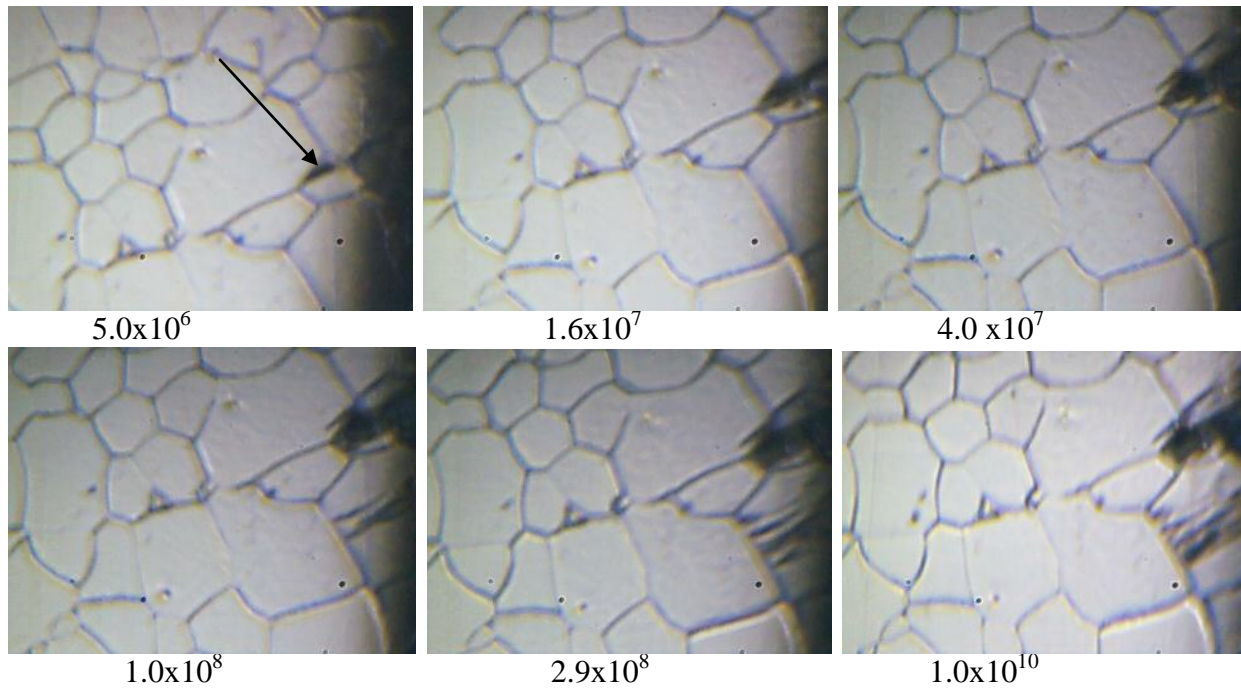


Fig. 4 Evolution of surface irreversible deformation under fatigue loading $\sigma_a=174$ MPa

Detail observations of surface irreversible slip bands or PSB under Scanning Electron Microscope (SEM) are given in Fig. 5. PSBs are found in 5 grains, where other grains remain undeformed at all. As described in f.c.c material, PSB formed by fatigue is localized irreversible plastic deformation. PSB is significantly changing the roughness of the original surface. At extrusion area, PSB lies to the mass of matrix out of the surface. At observation site, there are two main orientations of PSB at different grains whose PSB orientations have angle close to 90° . Even in similar orientation, the PSB have clear end at grain boundary. It suggests that PSB is anchored at grain boundary. PSB could active slip system in neighbor grain by enforce the stress concentration at inter boundary, but not go across the grain boundary. In the EBSD observation, same slip band direction always in the similar oriented grain (see slip band in red grain and orange grain). When neighbored grains have big difference in crystalline orientation, direction of slip band in different grain intents to be perpendicular (see slip band in red grain and blue grain). Unlike straight PSBs find in the f.c.c. crystalline, irreversible slip bands in b.c.c. are formed less individual.

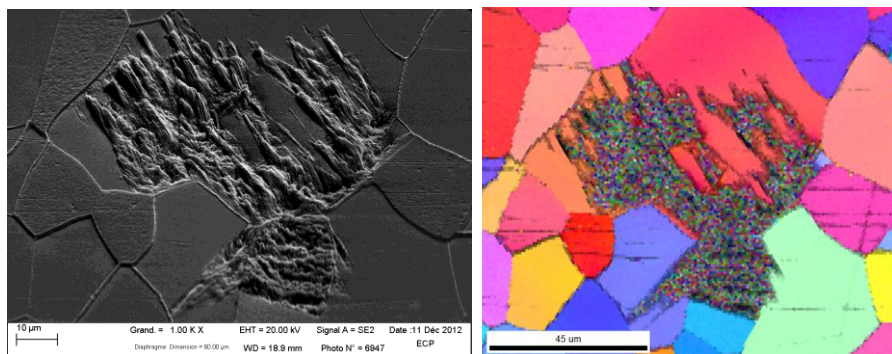


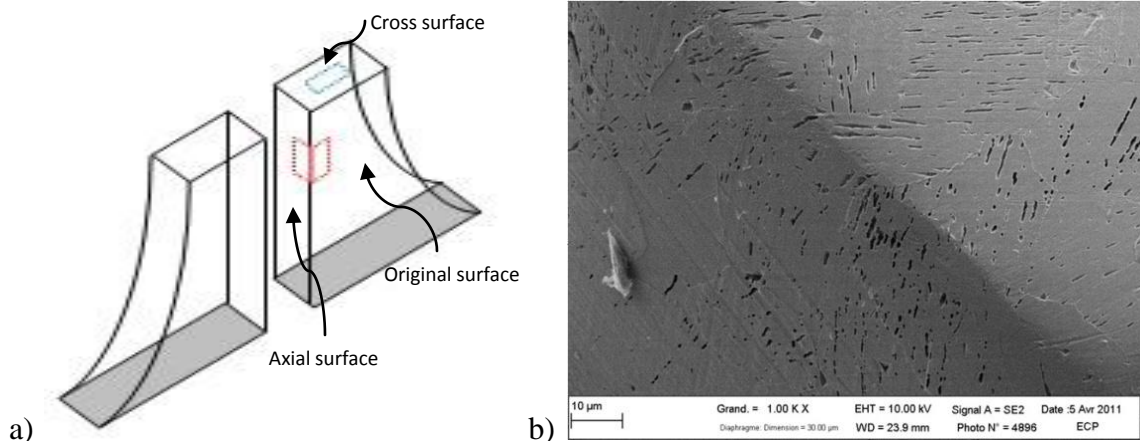
Fig. 5 PSB surface observation by SEM and EBSD

A specimen with pronounced PSBs was investigated in 3 perpendicular surfaces to have deeper understanding in 3 dimensions of PSB. The 3 surfaces are: original specimen surface, axial cutting surface and cross cutting surface as shown in Fig 6a. All 3 surfaces were prepared by carefully mechanical polish and 4% Nital etching. SEM observations at corner between axial cutting surface and original surface are presented in the Fig 6 b&c and cross section surface in the Fig 6d. Different oriented longitudinal slots were found pronouncedly at both side of corner on the axial cutting surface and original surface. Slots orientation changing takes place at grain boundary. It is reasonable to relate those slots to formation of PSB on the original specimen surface.

The figure 6c is the original surface observed with the inlens detector. It is easier to see, that the slots are not deep. It seems these slots are like cylinders. The width of each individual slot is around $0.5\ \mu\text{m}$, the distance between parallel slots varied from $1\ \mu\text{m}$ to $3\ \mu\text{m}$ and the length of slot is between $2\ \mu\text{m}$ to $10\ \mu\text{m}$.

On the cross section (Fig. 6d), it appears equiaxe hollows separated or not by a thin wall of matrix (in nanoscale). Hollows are distributed linear in several lines as marked in the yellow square (Fig. 6d). Those lines with hollows are parallel. Equiaxe hollow has size in $0.5\ \mu\text{m}$. Hollow lines observed here have length about $3\ \mu\text{m}$ to $5\ \mu\text{m}$. The distance between hollow lines is approximate $2\ \mu\text{m}$. Regarding this hollow deformation at cross section and longitudinal slots found in Fig 6c, it may be constructed a 3D schematic figure of the slots and hollows as Micron Abreast Pipes in Fig.6e

However in the fundamental material like ferrite, subsurface irreversible deformation is decreasing according plane stress condition function with distance to the surface



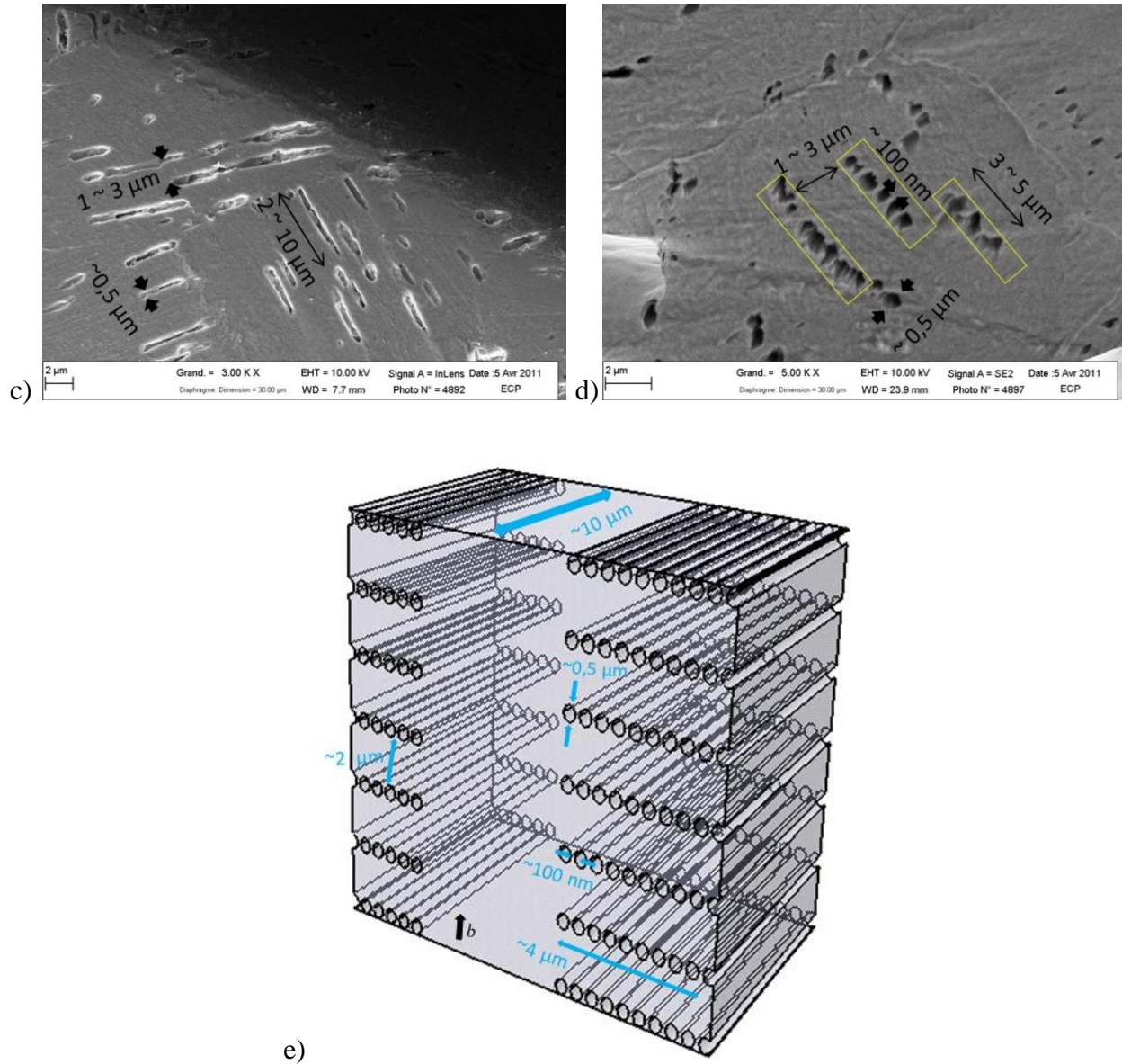
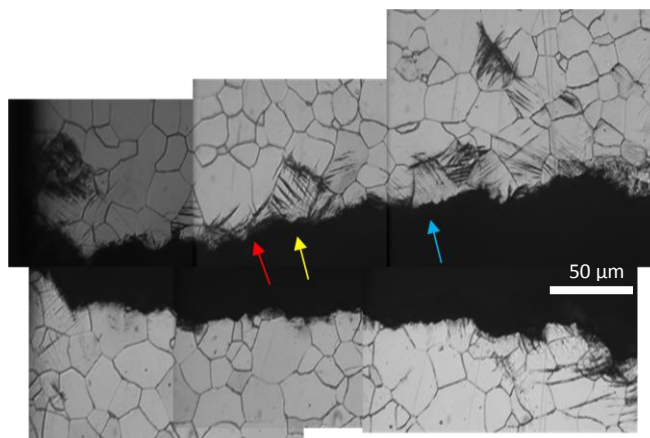


Fig. 6 slots after polish and etching the PSB [13] and micron scale channel in matrix



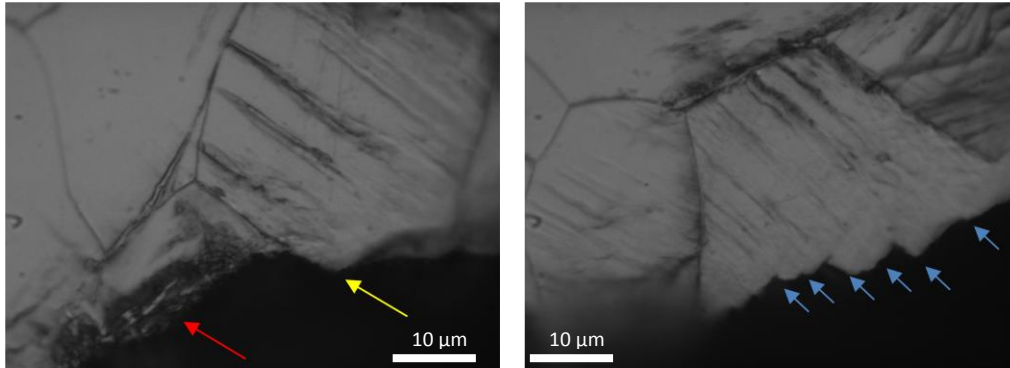
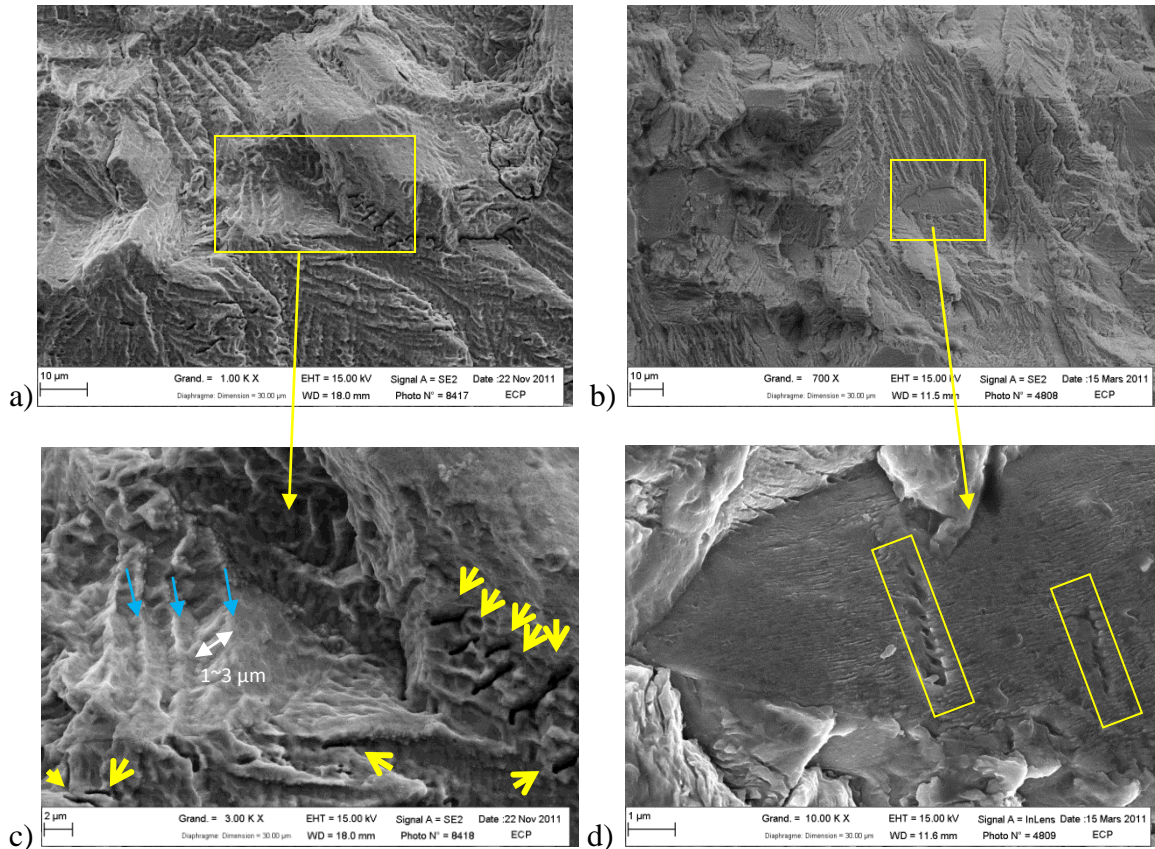


Fig. 7 Surface of cracked specimen

Surface microstructure observation after fracture shows as in Fig.7. Red arrow indicates a grain which has PSBs in it. In this PSB grain, crack opens along the PSBs which formed long time before crack occurs in this grain. Yellow arrow indicates the crack along a grain boundary. Intergranular crack takes place at grain boundary between two grains whose PSB are perpendicular to each other. Blue arrows denoted a transgranular crack. Crack stairs in the surface of this grain correspond to the appearance of slip bands below the fracture surface.



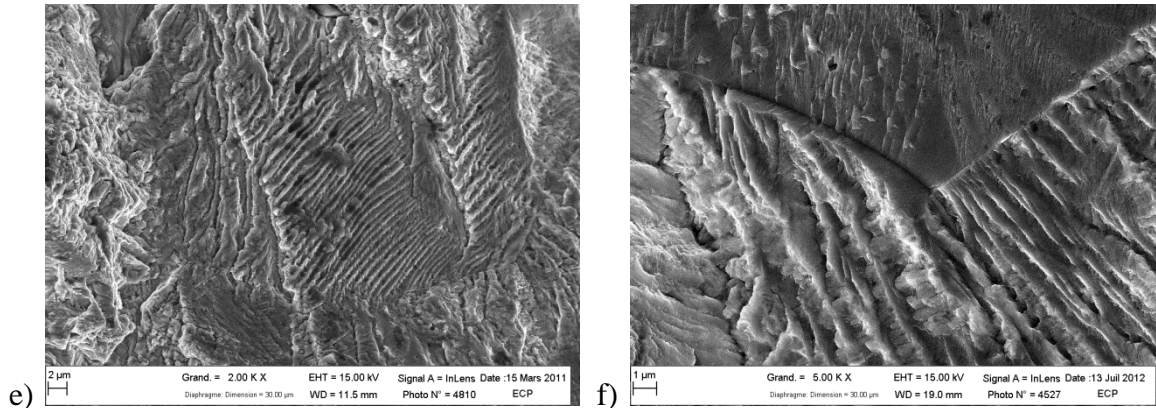


Fig.8 intergranular and transgranular crack at initiation area

Fracture surface gives more interesting results. In the initiation area, the grains trace is visible (Fig.8a and Fig.8b). Three types of pattern were found: one intergranular and two transgranulars. The intergranular pattern is seen in fig8b and 8d. This intergranular crack appears not smooth, but presents a very fine linear structure on the grain surface which believes related to the dislocation slips. Moreover, two lines of hollows separated by around $2 \mu\text{m}$ are visible (Fig. 8d). The first transgranular crack is shown in Fig. 8a and Fig.8c. The fracture surface through the grain is developed as a staircase. The distance between two stairs is about $2 \mu\text{m}$. It suggests the same mechanism that those forming the stair structure in the surface as blue arrows in Fig.7. The second pattern of transgranular crack is shown Fig.8e or Fig.8f (where a transition from an intergranular crack to the second transgranular pattern is seen). In this transgranular case, the fracture surface is composed of longitudinal pipes arranged side by side. The diameter of the pipes is $0.6\mu\text{m}$ in average. It may be correspond to PSB on the surface indicated by red arrows in Fig.7.

Now, it is interesting to relate the fracture surface pattern with the subscale damage produced by PSB as Micron Abreast Pipes seen in Fig.6. An illustration of this fracture mechanism is schematically reported on the Fig. 9. The staircase structure is probably a fracture occurring partially on abreast pipes, and crossing over to abreast pipe just below or above. The distance between two stairs is about $2 \mu\text{m}$, in good agreement with the distance between two abreast pipes. In the case of second transgranular pattern, the crack path is entirely on abreast pipes in the same dislocation slip plane. The characteristic dimension of this pattern is pipe diameter about $0.5 \mu\text{m}$. The line of hollows (separated in distance $2 \mu\text{m}$) seen on the intergranular surface Fig 6d are probably the end of abreast pipes at grain boundary (in good agreement with the distance between two neighbored pipes). However, abreast pipes sometime may linked through the nanoscale wall between pipes to form subscale 2 dimensions planar default as small facets denoted by yellow arrows in Fig 8c.

As shown previously (Fig.6 and 8), irreversible slip band not only take place on the surface but also at subsurface (with a minor density). The internal irreversible plastic deformations will potentially facilitate the fatigue crack initiation. Then it can conclude here that very high cycle fatigue crack initiate not only by extrusion and intrusion, but also due to irreversible slip bands in the subsurface. It starts from the irreversible slip bands in the surface, which induces stress

concentration and produces the occurrence of PSB in subsurface [13]. Then irreversible slip bands in the subsurface makes easier the fatigue crack initiation stage. Fatigue crack at subsurface at initiation stage is form by connecting subscale defaults, such as Micron Abreast Pipes in same slip plane, inharmonious of deformation at grain boundary or links between small facets of irreversible slip bands.

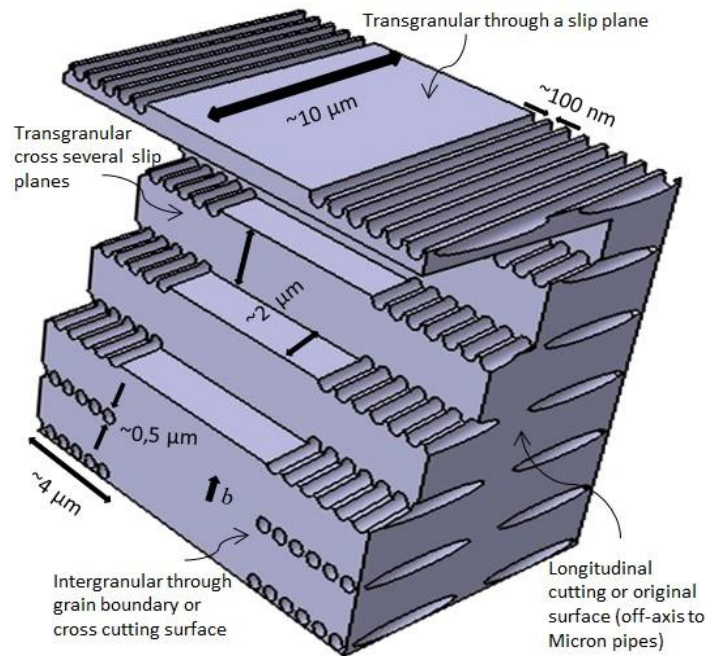


Fig. 9. Fatigue crack at initiation area relative to PSB in material

Regarding fatigue propagation threshold and temperature elevation [14,15], it may estimate following mechanism of fatigue initiation in ferrite at VHCF regime. PSB occurs on specimen surface at beginning stage of VHCF test. With following loading cycles, more PSBs formed in surface and subsurface, evidently at location of initiation area. In means material volume in a small initiation area is damaged by PSB but not opened by a crack. PSBs and other multiplied dislocation lines make more volume at initiation area extended and weak to undertake the long range stress. Therefore pronouncedly stress concentration takes place in front of area extended. Consequently extended area grown to the edge of initiation area which correspond to the fatigue stress intensity factor threshold $\Delta K_{th} = E\sqrt{b}$ (Herzberg-Paris-McClintock law) [16]. By sufficient stress concentration, the initiation area opened suddenly and remained some area in initiation cracked without plastic deformation. As blue arrows in Fig 7, between two slip planes, crack at stairs shows no plastic deformation on surface. The temperature recording [14] of VHCF test has shown that the crack initiation stage occurs at the end of VHCF test (less than 1% of the total life). More than 99% of the total life is takes up by the micro-damage due to forming PSBs in surface and subsurface, especially initiation area. The first fatigue crack appears on the specimen surface, the entire crack initiation zone appears supervening by connecting all defaults in the bulk material with in short time at end of VHCF.

4. Conclusions

According to the results described above, the following conclusions may draw for ferrite material failed in VHCF:

- 1) Irreversible deformation (PSB) forms on the surface specimen at the beginning stage of VHCF in plane stress condition
- 2) Irreversible deformation can grow or multiplies independently at neighbor grains. After 10^9 cycles new irreversible deformation (localized plastic strain) per each loading cycle $\Delta\epsilon/N$ is decreasing by increasing number of cycle.
- 3) Irreversible deformation not only exists on the surface before crack but also in the subsurface volume.
- 4) Irreversible plastic deformations at subsurface makes easier the fatigue crack initiation.

Acknowledgements

This research was supported by the grant from the project of Microplasticity and energy dissipation in very high cycle Fatigue (DISFAT, project No. ANR-09-BLAN-0025-09), which funded by the National Agency of Research, France (ANR). Inner discussions of DISFAT project with Prof Mughrabi and other members are great appreciated here. The authors also thank F.Garnier for her participation of SEM observations.

References

- [1] S. Suresh, Fatigue of materials (second edition), Cambridge university press, Cambridge, 1998
- [2] Bathias, C., Pineau, A. Fatigue des matériaux et des Structures, 2008, pp85-246
- [3] Mughrabi, H. The Strength of Metals and Alloys, pp.1615-1639, Haasen, P., Gerold, V., Kostorz, G., (Ed.), Pergamon Press, Oxford, 1980
- [4] H. Mughrabi, Microscopic mechanisms of metal fatigue, Strength of Metals and Alloys, 3 (1979), pp. 1615-1638
- [5] Mughrabi, H., Herz, K., Stark, X. (1976) Int Journal of Fracture 17, 193-320
- [6] Mughrabi, H., Wüthrich, Ch. (1976) Philosophical Magazine A33, 963-984
- [7] Mughrabi, H., Ackermann, F., Herz, K. (1979) In: ASTM STP 675, pp 69-105
- [8] Klesnil, M., Lukas, P. (1965) J. of the Iron and Steel Institute 203, 1043 – 1048
- [9] Sommer, C., Mughrabi, H., Lockner, D. (1998) Acta Mater. 46, 1527-1536
- [10] J.T. Mcgrath, W.J. Bratina, Dislocation structures in fatigued iron-carbon alloys, The Philosophical Magazine, 12, 1293-1305, 1965.
- [11] Wood, W. A. ; Reimann, W. H. ; Sargant, K. R. Comparison of Fatigue Mechanisms in Bcc Iron and Fcc Metals, Transactions of the Metallurgical Society of AIM vol. 230, 511-518, 1964.
- [12] R. P. Wei, A. J. Baker, Observation of dislocation loop arrays in fatigued polycrystalline pure iron, Philosophical Magazine, vol.12, 1087-1091, 1965
- [13] C. Wang, D. Wagner, Q.Y. Wang, C. Bathias. Gigacycle fatigue initiation mechanism in Armco iron, International Journal of Fatigue, Volume 45, December 2012, Pages 91-97
- [14] Chong Wang, Danièle Wagner, Claude Bathias - Study of fatigue crack mechanism on an armco iron in the gigacycle fatigue by temperature recording and microstructural observations, Abstract paper accepted at ICF 13
- [15] N. Ranc, D. Wagner, P.C. Paris – Study of thermal effects associated with crack propagation during very high cycle fatigue, Acta Materiala 56 (2008) 4012-4021.
- [16] Claude Bathias, Paul C. Paris. Gigacycle fatigue of metallic aircraft components. International Journal of Fatigue, Volume 32, Issue 6, June 2010, Pages 894-897